

# IMPROVEMENT OF STABILITY OF BRIDGE BY USING BEARING

Sushant<sup>1</sup>, Omkar<sup>2</sup>, Nilkanth<sup>3</sup>,

*1 Sushant Balu Bhosale, Department of Civil Engineering , Jaihind College of Engineering Kuran Pune, Maharashtra, India*

*2 Omkar Suresh Bhagawat, Department of Civil Engineering , Jaihind College of Engineering Kuran Pune, Maharashtra, India*

*3 Nilkanth Devidas Darekar, Department of Civil Engineering , Jaihind College of Engineering Kuran Pune, Maharashtra, India*

*Guide By,*

*Prof. Zope M.T., Department of Civil Engineering, Jaihind College of Engineering, Kuran Pune, Maharashtra, India*

## ABSTRACT

To find out if and how A set of 1 g shaking table tests were carried out to determine how much the integration of the girder, abutments, and backfill may improve the seismic stability of already constructed bridges. The following three categories of little bridge models were put to the test:(1) the conventional type, which consists of a beam supported by two gravity supports (without a pile foundation) by means of fixed and movable bearings; (2) integrated beam and supports; and (3) reinforced backfill, which is formed by two layers of large-diameter nails attached to both the top of the abutment and its toe or heel. (A series of 1 g shaking table experiments were performed to find out if and how combining girder, abutment, and backfill may greatly boost the seismic stability of existing bridges. The trio of kinds of small model bridges that were tested are:(1) conventional type, consisting of two beams supported by gravity-type piers (without pile foundations) supported by fixed and movable bearings.(2) An integrated girder and abutments.

## 1. INTRODUCTION

Tokyo University of Science contributed money for this research. The Japan Railway Technical Research Institute conducted the shaking table experiment. We are appreciative that the Tokyo University of Science Master of Science program was funded by the Inter-American Development Bank (IDB) for the second author. This money was made possible through the Japan-IDB in the Scholarship of a Program.

## 2. PROBLEM STATEMENT & AIM

Unreinforced backfill can lead to the dynamic collapse of the backfill surface and projection of the completely expanded soil, which can cause critical bridges of the conventional type to occur. The impact of the bullet causes

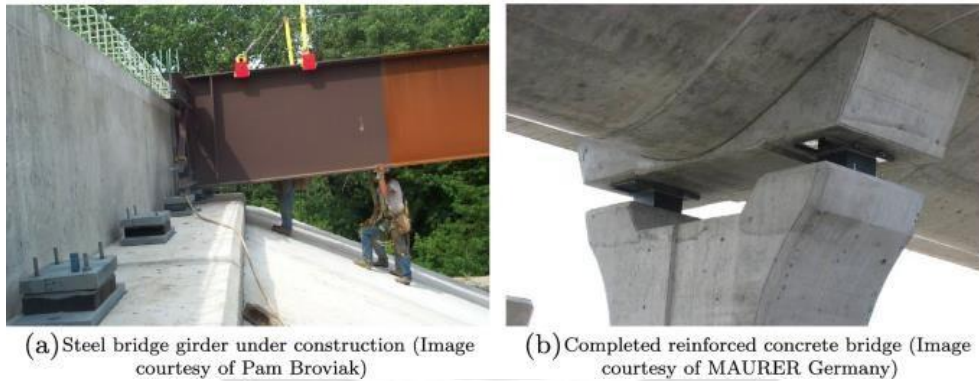
cyclic lateral motions due to the heated stretching and retraction of the support on a periodic basis. However, after that, GRS bridges essentially don't have these issues. First, the filler's dynamic frustration is limited by the reinforcing layers that are bound against one another. The pavement must be able to distribute efficiently under the impact of a huge soil mass since it acts as a continuous column with a limited span, supported by many support layers, also known as reinforcement layers.



**Fig -1**

### 2.2 Objective of the project:

1. To investigate the bridge's stability in Jaihind Campus utilizing a variety of bearings.
2. To determine an appropriate bearing in a bridge



(a) Steel bridge girder under construction (Image courtesy of Pam Broviak)

(b) Completed reinforced concrete bridge (Image courtesy of MAURER Germany)

**Fig -2**

### 3. METHODOLOGY:

#### 1. Bridge types

The end of a beam resting on a moving bearing and unreinforced infill are particularly unstable under seismic stress; conventional bridges frequently have extremely low dynamic stability. By incorporating the girder inside the boundaries of conventional integral bridge types, some of these and other issues related to conventional bridges can be mitigated. Unreinforced fill still has certain limitations when it comes to seismic stability. Some of these issues with GRS RW bridges can be resolved by adding geosynthetic reinforcement layers at the back of the FHR to strengthen the fill.

strong initial natural frequency, low rate of natural frequency decay under dynamic loading, strong dynamic strength against rebound, and high energy dissipation capacity all contribute to the excellent dynamic stability of GRS integrated bridges.

## 2. Shaking Table

This study used the same methods as Tatsuoka et al. extensively described for the shake table testing, in addition to fastening the backfill and providing soil support with large-diameter model nails. As such, this is only a synopsis. were conducted on small-scale models of conventional bridges with five different types of reinforcement and conventional bridges with a single beam that is simply supported and two filled, gravity-type sockets that are not reinforced.

## 3. Conventional type bridge (CB)

The model is a single-span bridge with two gravity-type supports, an unreinforced infill, and a beam supported by two fixed and moveable bearings. The left end of the beam was able to slide horizontally thanks to the movable linear motion bearing, while the right end was able to rotate thanks to the fixed lever bearing. Consequently, asymmetric dynamic behavior results from the right support of model CB being dynamically less stable than the left support.

Use a 2 m long model beam to replicate a prototype that is 20 m long. For this and subsequent models with a relative density of  $D_r$ , air-dried Toyoura sand ( $e_{max} = 0.970$ ,  $e_{min} = 0.602$ ,  $G_s = 2.65$ ,  $U_c = 1.64$ , and  $D_{50} = 0.179$  mm) was cut to construct the base and fill. the filling. To regulate filling deformation, many tiny circular targets and horizontal layers of black-dyed sand, 7 mm thick, were positioned on the right abutment and filled 10 cm vertically just beneath the glass window.

## 4. Dynamic loading

Remaining Motion and Distortion The six bridge models' right support residual motions that were seen at the conclusion of their corresponding loading stages are depicted. For a fair comparison, these transitions are displayed as a function of the basic acceleration  $\alpha_b$  in individual steps rather than the response acceleration, which changes by the same  $\alpha_b$  in these numerous models. Because the amplitude of the basic acceleration ( $\alpha_b$ ) was not maintained absolutely, the value of  $\alpha_b$  was used for these plots.

Earth pressure lateral vertical distributions behind the model's right abutment. Similar to the right and left limitations, their distributions peak when the beam is greatest displaced in the active and passive directions.

## 5. Dynamic behavior as a damped SDOF system

Due to the particular dynamic loading method used in each shaking table test described in this work, the failure started at resonance and gradually increased in the fundamental level. Because of the particular dynamic loading method used in each shaking table test described in this work, the failure started at resonance and was gradually increased with respect to the fundamental acceleration ( $\alpha_b$ ) at  $f_i = 5$  Hz. As a result], the initial value  $\beta = f_i/f_0$  was still less than unity in comparable shaking table experiments (Muñoz et al., 2012, Tatsuoka et al., in press) when  $f_i$  was changed from 2 to 20 Hz. didn't begin On the other hand, at  $f_i = 20$  Hz, the resonant condition was quickly surpassed before  $\alpha_t$  achieved the value at which failure began at  $f_i = 5$  Hz.

When the initial (undamaged) stiffness of a bridge system increases,  $f_0$  rises and the initial value  $\beta = f_i/f_0$  decreases to less than unity. In such scenario, the chance of failure for a certain load history acceleration ( $\alpha_b$ ) at  $f_i = 5$  Hz is decreased along with the damage in the bridge system and the initial reaction and acceleration magnification ratio (M). Because of this, the starting value  $\beta = f_i/f_0$  remained less than unity in comparable shaking table experiments where  $f_i$  was changed from 2 to 20 Hz. didn't initiate In contrast, at  $f_i = 20$  Hz, the failure started at  $\alpha_t = 5$  Hz, and the resonance condition was attained before it passed swiftly. Dynamic ductility

In response to increased dynamic ductility, the bridge system softens more slowly with increased loading cycles and input acceleration level. This lowers the likelihood of reaching the resonance state, which is the potential beginning point of failure. The softening rate often rises as the resonance state approaches, increasing the likelihood of both failing to initiate and failing to achieve the resonance state. After reaching the resonance stage, if the intense shaking persists, there's a chance that the  $\beta$  value may rise and a complete collapse will occur. On the other hand, because the  $\beta$  increases and the resonance state approaches more slowly, the response stays small and decreases when the dynamic ductility reaches a significant level.



### Damping ratio ( $\xi$ ) at failure

In the event that PGA materializes, the design reaction acceleration at the girder ( $\alpha t$ ) for a given design earthquake motion is equal to the design peak horizontal ground acceleration (PGA) times the magnification ratio ( $M$ ). When  $\beta = \beta$  resonance, the highest value of  $\alpha t$  in this study corresponds to ( $\alpha t$ ) resonance =  $M$  peak times ( $\alpha b$ ) resonance. As the damping ratio,  $\xi$ , at resonance increases, the  $M$  peak value drops. Conversely, it tends to rise in tandem with an increase in dynamic strength, often known as ( $\alpha t$ ) resonance or the acceleration of response at resonance. These four variables serve as the foundation for evaluating the dynamic behavior of the four bridge models. It is demonstrated that each of these components is increased by the integration of the girder, abutments, and backfill.

### Overall dynamic behavior of the four models

The correlations between  $\alpha t$  and the back-calculated tuning ratio,  $\beta = f_i/f_0$ , are displayed. This graph and similar ones don't show the data during the first cycle, when the reaction is clearly cyclical. In all cases, at first,  $\alpha t$  was not much more than  $\alpha b$ , and as  $\alpha b$  increased,  $\alpha t$  came to be larger than  $\alpha b$ . Second, when  $\beta$  got closer to unity, the biggest  $\alpha t$  happened. Following the resonance state,  $\alpha t$  dropped but  $\alpha b$  stayed same. Not only that, but in these models, as dynamic strength grew, the rate of  $\beta$  reduced, and as loading cycles increased, the rate of  $\beta$  increased. In other words, the resonance state was attained more slowly as  $\alpha b$  grew as the dynamic strength increased.

### Conventional type bridge (CB)

The back-calculated tuning ratio  $\beta = f_i/f_0$  and its connection with  $\alpha t$  are presented. There is a clear temporary reaction in the first cycle, but this graph and others of a similar kind do not show the outcomes.  $\alpha t$  was not significantly bigger than  $\alpha b$  at first for any model, and when  $\alpha b$  increased,  $\alpha t$  came to be greater than  $\alpha b$ . Furthermore, when  $\beta$  got closer to unity, the greatest  $\alpha t$  was seen. While  $\alpha b$  was steady,  $\alpha t$  saw a drop after passing the resonance stage. In these models, it is worth noting that the rate of  $\beta$  rose with a rise in loading cycles, but it dropped with an increase in dynamic strength. That is, the resonance state was achieved more slowly as  $\alpha b$  grew, but at a higher dynamic strength.

### Integrated conventional type bridge (CB-L)

The  $M$  and  $\beta$  values increased from their starting points,  $M=1.04$  and  $\beta=0.20$  (at the start of stage I), to the values at the start of failure,  $M_{peak}=1.51$  and  $\beta_{resonance}=0.98$ , when ( $\alpha b$ ) resonance = 606 gals at stage VII (Fig. 17(a)). At this stage, the L-shaped metal fixtures started to yield substantially, and the footing advanced concurrently with the emergence of distinct shear bands in the backfill. Additionally, the tops of the abutments started to twist (Fig. 9(a)). In this case, the main cause of the bridge's decreasing stiffness is a decrease in factors (a). From the preceding list, (b) and (c). The mechanism that caused model CB-L to collapse and fail proceeded much more slowly than it did for model CB. In particular, the  $M$

This improvement in dynamic ductility is the result of the girder's interaction with the abutments. The transitory resonance was crossed in the latter cycles of stage VII as the number of cycles ( $N$ ) rose, and the value of  $M$  significantly decreased in association with the continual increase in the values of  $\beta$  and  $\phi$ . Eventually, the abutments rotated much, the L-shaped metal fittings gave greatly, and the abutment bottoms were entirely pushed out, resulting in the collapse condition. The coefficient of sub-grade response significantly decreased as a result of this break in contact between the abutment bottom and the supporting ground. In the end, the value of  $\beta$  increased well beyond unity. All of these circumstances should have resulted in a very low overall bridge rigidity.

## 4. PROBABLE CONCLUSIONS

The model test and analysis results shown above allow for the derivation of the following conclusions:

- Existing conventional-type bridges, which are made up of a girder that is simply supported by two abutments via two movable and fixed bearings, have much greater seismic stability when the backfill and supporting ground are secured with large-diameter nails fastened to the top and bottom of the abutments and integrated with the girder. The two factors contributing to the increase in seismic stability are (2) the increase in dynamic strength against response acceleration and the increase in the initial natural frequency ( $f_0$ ) of the bridge system to a value sufficiently higher than the predominant frequencies ( $f_p$ ) of major earthquakes, which lowers the initial response. where, by keeping the  $f_0$  value far higher than the  $f_p$  value, keeps the bridge's reaction far from resonance; (iv) A
- (3) Because of the girder's integration with the abutments, seasonal thermal expansion and contraction of the girder results in cyclic lateral displacements at the abutment top. Due to the double ratchet mechanism, there is a risk of significant active failure in the backfill with significant settlements, as well as a significant risk of severe passive

earth pressure buildup at the rear of the abutment. These adverse effects can be significantly mitigated by using large-diameter nails that are secured to both the top and bottom of the abutment. These are basically the benefits of integrated nail-reinforced soil (NRS) bridges.

## 6. REFERENCES

Muñoz & colleagues (2012)

H. Nishikiori, K. Watanabe, M. Tateyama, F. Tatsuoka, D. Hirakawa, R. Soma, and H. Muñoz

Dynamic stability of a geosynthetic fiber-reinforced integrative soil bridge

International Journal of Geosynthetics, Volume 19, Issue 1, Pages 11–38, (2012)

View the Scopus article that is cross-referenced. Google Scholar

Shinoda et al., consisting of F. Tatsuoka, T. Uchimura, and M. Shinoda, in 2003

Preloading and prestressed mechanically reinforced backfill using a ratchet connection to improve its dynamic performance 33–54 in *Soils and Foundations*, 43 (2) (2003)

